doi.org/10.26434/chemrxiv.9784082.v1

Two-Metal Ion Mechanism of DNA Cleavage in CRISPR-Cas9

Lorenzo Casalino, Martin Jinek, Giulia Palermo

Submitted date: 08/09/2019 • Posted date: 10/09/2019

Citation information: Casalino, Lorenzo; Jinek, Martin; Palermo, Giulia (2019): Two-Metal Ion Mechanism of DNA Cleavage in CRISPR-Cas9. ChemRxiv. Preprint.

CRISPR-Cas9 is a cutting-edge genome-editing technology, which employs the endonuclease Cas9 to cleave DNA sequences of interest. However, the catalytic mechanism of DNA cleavage and the critical role of the Mg^{2+} ions have remained elusive. Here, quantum–classical QM(Car-Parrinello)/MM simulations are used to disclose the two-Mg^{2+} aided mechanism of phosphodiester bond cleavage in the RuvC domain. We reveal that the catalysis proceeds through an associative pathway activated by H983 and fundamentally assisted by the joint dynamics of the two Mg^{2+} ions, which cooperatively act to properly orient the reactants and lead the chemical step to completion. Cross-validation of this mechanism is achieved by evaluating alternative reaction pathways and in light of experimental data, delivering fundamental insights on how CRISPR-Cas9 cleaves nucleic acids. This knowledge is critical for improving the Cas9 catalytic efficiency and its metal-dependent function, helping also the development of novel Cas9-based genome-editing tools.

File list (1)

Two-metal ion mechanism of DNA cleavage in CRISPR-Cas9

Lorenzo Casalino,[1] Martin Jinek[2] and Giulia Palermo[3*]

1. Department of Chemistry and Biochemistry, University of California San Diego, La Jolla, CA 92093, United States

2. Department of Biochemistry, University of Zürich, Winterthurerstrasse 190, CH-8057 Zürich, Switzerland

3. Department of Bioengineering and Chemistry, University of California Riverside, 900 University Avenue, Riverside, CA 92521, United States

Corresponding Author

Dr. Giulia Palermo, giulia.palermo@ucr.edu

Abstract

CRISPR-Cas9 is a cutting-edge genome-editing technology, which employs the endonuclease Cas9 to cleave DNA sequences of interest. However, the catalytic mechanism of DNA cleavage and the critical role of the Mg^{2+} ions have remained elusive. Here, quantum–classical QM(Car-Parrinello)/MM simulations are used to disclose the two-Mg^{2+} aided mechanism of phosphodiester bond cleavage in the RuvC domain. We reveal that the catalysis proceeds through an associative pathway activated by H983 and fundamentally assisted by the joint dynamics of the two Mg^{2+} ions, which cooperatively act to properly orient the reactants and lead the chemical step to completion. Cross-validation of this mechanism is achieved by evaluating alternative reaction pathways and in light of experimental data, delivering fundamental insights on how CRISPR-Cas9 cleaves nucleic acids. This knowledge is critical for improving the Cas9 catalytic efficiency and its metal-dependent function, helping also the development of novel Cas9-based genome-editing tools.

Introduction

CRISPR (clustered regularly interspaced short palindromic repeats)-Cas9 is a revolutionary genome-editing tool, which is enabling innovative discoveries across the fields of biomedicine, pharmaceutics, biofuel production and agriculture.[1,2] This system uses the RNA-guided endonuclease Cas9 to precisely cleave DNA sequences of interest.[3] However, the catalytic mechanism of DNA cleavage, which is a fundamental step for the editing of the genome, is not completely understood. In the activated form of the enzymatic complex, two catalytic domains – RuvC and HNH – perform the cleavage of the DNA strands through a metal (Mg^{2+})-aided function (Figure 1A).[2,4] The RuvC domain shares the structural fold of the RNA Ribonuclease H (RNase H) and – as it occurs in this latter – is thought to perform phosphodiester bond cleavages through a two-metal-ion mechansms.[5,6] However, the mechanistic details of the catalysis remain elusive. The RuvC active site hosts three carboxylates (D10, D986 and E762), which coordinate the two catalytic metals (Figure 1B) and constitute the highly conserved DDE (or DEDD) motif of the two-metal-dependent nucleases.[6–9] The H893 residue projects into the active site, suggesting a possible role in the catalysis.[7] Previous computational studies employing extensive classical molecular dynamics (MD),[10–12] revealed that solvation waters surround the active site, while one water molecule stably coordinates the A-site ion (MgA), acting as a possible nucleophile (Figure 1B). In this scenario, critical open questions concerning the mechanism of non-target DNA cleavage, such as the origin of the nucleophile initiating the chemical step, and the mechanism type leading to the actual cleavage remain unmet. The efficiency and specificity of the enzyme dep nds on these and on other unresolved mechanistic aspects, such as the pivotal role and the dynamics of the catalytic metals.[13] Their understanding is crucial to improve the enzyme specificity and reduce off-target cleavages, a key goal of biomedical applications of CRISPR-Cas9 genome-

editing.[1,14] Here, we investigate the mechanism of phosphodiester bond cleavage in RuvC through extensive (i.e. ~480 ps) quantum−classical QM(Car−Parrinello)/MM MD simulations (*ab-initio* MD),[15,16] performed on different starting configurations, to explore alternative pathways. The calculations reveal an associative catalysis activated by the H983 side-chain, and fundamentally assisted by the joint dynamics of the metal ions. The mechanistic details of this two-metal aided catalysis described here provide foundational information for improving the CRISPR-Cas9 catalytic efficiency and its divalent metal-dependent activity.

Results and Discussion

Conformation of the Reactant. QM/MM MD simulations have been carried out by treating the active site at the DFT-BLYP[17,18] level, into an overall MM box of ~340,000 atoms. The QM part (115 atoms) includes the scissile and adjacent DNA phosphates groups, the metal ions and the DDE coordinating residues, as well as H983 (protonated in epsilon, as arising from a number of investigations)[6,12] and six solvation waters (see the Supporting Information (SI)). Notably, *ab-intio* MD has been performed substituting the crystallized Mn^{2+} ions with the catalytically active Mg^{2+} ions.[6] During unconstrained *ab-initio* MD (two replicas of ~40 ps), the DDE motif steadily coordinates the Mg^{2+} ions, while the H983 nitrogen detaches from MgA, whose coordination sphere is saturated by the side-chain oxygen of S13 (Figure 1C and S1). Simultaneously, the nucleophilic water molecule coordinating MgA moves in between H983 and the scissile phosphate, positioning itself for the chemical reaction. This configuration is stable during additional ~40 ps (Figure S1). The detachment of the H983 ligand from MgA is not surprising, as also observed during classical MD studies.[11,12] Indeed, Mg^{2+} poorly binds to nitrogen, whereas Mn^{2+} shows high affinity[17,18] for nitrogen atoms in crystallization buffers.[19]

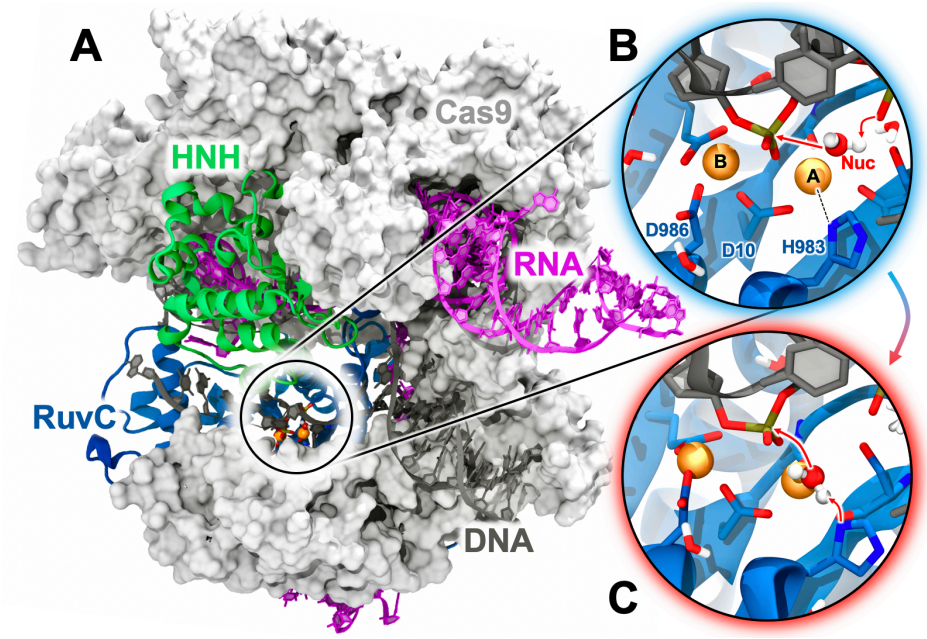

Figure 1. (a) Overview of the CRISPR-Cas9 complex bound to a guide RNA (magenta) and to a target DNA (black). Cas9 is in molecular surface, highlighting the HNH (green) and RuvC (blue) domains. **(b)** Inset of the RuvC active site, displaying the catalytic metals (A and B, orange), the surrounding protein residues and water molecules. **(c)** Configuration of the active site, as arising from *ab-initio* molecular dynamics.

However, the native Mg^{2+} ions are unlikely to preserve the nitrogen ligand, as shown in several two-metal-dependent enzymes.[20] To cross-validate this observation within the RuvC site, we performed unconstrained *ab-initio* MD in the presence of the crystallographic Mn^{2+} ions, revealing that MnA preserves the nitrogen ligand over ~40 ps (Figure S2). This indicates that the coordination of MgA by means of H893 is unlikely in the RuvC site. The water nucleophile locates in between H983 and the scissile phosphate, positioning for the chemical reaction. Yet, H983 interacts with the attacking water, which in turn is positioned in proximity to the scissile

phosphate and coordinates MgA (Figure 2B). The resulting stable configuration of the reactant lays the foundation for investigating the catalytic mechanism.

Mechanism of phosphodiester bond cleavage. To probe the mechanism of phosphodiester bond cleavage, we performed QM/MM MD free energy simulations, employing thermodynamic integration and the *"blue moon ensemble"* method (see the SI).[21] The reaction step has been investigated using as a reaction coordinate (RC) the difference in distance between the breaking ($O3'_{DNA}$–P_{DNA}) and forming (O_{WAT}–P_{DNA}) bonds (Figure 2). The appropriateness of this approach and of the employed RC for phosphodiester bond cleavage has been shown in several studies of RNA/DNA processing enzymes,[22–24] including our recent contributions (discussion in the SI).[25,26] As noted earlier, this RC does not specify *a priori* the group accepting a proton from the attacking water, allowing an unbiased representation of this key step.[23] QM/MM free energy simulations (~160 ps of aggregate sampling) show that the system evolves from the reactant (**R**) to the products (**P**), separated by a transition state ($\mathbf{TS}^{\ddagger}$) maximum (Figure 2A). The reaction is activated by H893, which acts as a general base, and proceeds through an associative S_N2 mechanism. In detail, at a RC = 0 Å, a proton transfer (**PT**) event is observed, as the water molecule releases the proton to His893, activating the hydroxide ion. Notably, the PT event occurs right before and is barrier-less with respect to the $\mathbf{TS}^{\ddagger}$. Upon activation, OH^- becomes aligned with the scissile P–O3' bond, resulting in the formation of $\mathbf{TS}^{\ddagger}$. At RC = 0.4 Å, the reaction evolves downhill toward **P** formation. A full description and cross-validation of this mechanism, including hysteresis calculation and $\mathbf{TS}^{\ddagger}$ analysis, is given in the SI. The process of phosphodiester bond cleavage shows a Helmholtz free energy (ΔF#) of ~17 kcal/mol, in line with the experimental catalytic rate corresponding to ΔG# ~16 kcal/mol.[27] This rate constant has been measured distinguishing the catalysis from nucleic acid binding and providing a measure for the RuvC do-

main, enabling proper comparison with our computations. Biochemical experiments showing the abolishment of the RuvC activity when H983 is mutated into alanine support the active role of H983 in the catalysis evinced in our simulations.[7] The variation of the significant distances along the reaction step (Figure 2B) provides insights on the role of the Mg^{2+} ions. At **TS**‡, the two Mg^{2+} ions are brought closer and the pro-Sp (O_{Sp}) oxygen approaches MgB. This is consistent with the two-metal-ion catalysis,[5,13] where the two metals cooperatively coordinate the reactant groups and stabilize **TS**‡. During multi-ps dynamics from **R** to **TS**‡, MgA stably locates in close contact to the water's oxygen. In this way, MgA acts as a Lewis acid, properly orienting and activating the nucleophile. Subsequently (from **TS**‡ to the **P**), MgA detaches from the OH group, while MgB stably interacts with O3', facilitating its exit as leaving group.

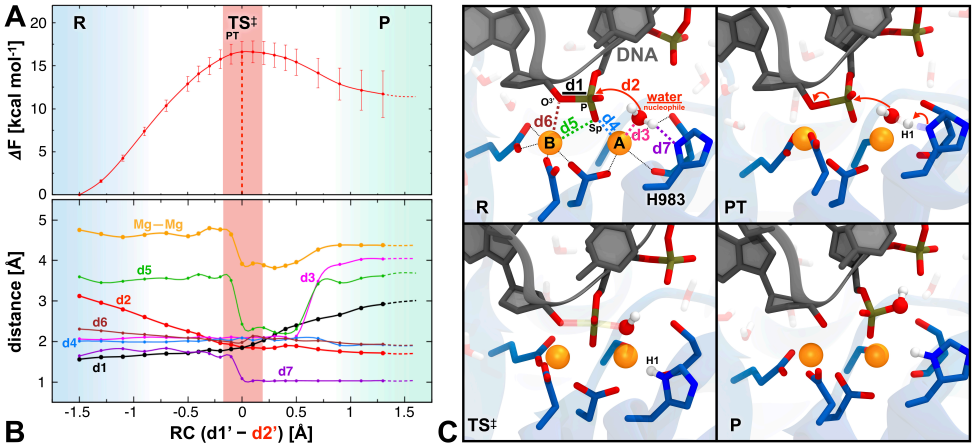

Figure 2. Structural and energetic properties for the two-Mg^{2+} aided catalysis in CRISPR-Cas9. **(a)** Free energy profile (ΔF#, top) and **(b)** selected bond distances (shown in panel (c)), computed along phosphodiester bond cleavage. The difference in distance between the breaking and forming P–O bonds is used as a Reaction Coordinate (RC). The Reactant (R), Proton Transfer (PT), Transition State (TS‡) and Product (P) regions are highlighted using colored bars. **(c)** Snapshots of the R, PT, TS‡ and P states.

Alternative Reaction Pathways. To examine the possibility of alternative reaction pathways, we performed *ab-initio* MD on different initial configurations of the RuvC site. In the Mn^{2+}-bound structure of CRISPR-Cas9 (Figure 1B),[2] H983 does not directly interact with the attacking water, which could be activated by a different mechanism. QM/MM MD free energy simulations starting from this configuration (details in the SI) reveal a dissociative S_N1 reaction pathway (Figure 3, Movie S2). In this mechanism, the dissociation of the leaving group (O3') is reached at the TS‡', while the water nucleophile is converted into OH^- through a proton transfer (PT') to the adjacent phosphate only after the formation of the O_{WAT}–P_{DNA} bond has started (full description and cross-validation in the SI). The computed ΔF# reaches > 18 kcal/mol, which is unfavorable compared to the associative pathway activated by H983 (Figure 3). Here, MgA does not act as a Lewis acid, as it loosely binds the attacking water (Figure S3). Rather, it activates the electrophile (i.e. the scissile phosphate), while MgB stabilizes the oxyanion leaving group. Such a dissociative mechanism is rare in the two-Mg^{2+}-dependent enzymes[28–30] and, considering the increased ΔF# compared to the H893-activated catalysis (Figure 2), it appears less likely for the RuvC catalysis. A third configuration of the RuvC site has also been object of *ab-initio* MD, ruling out other potential reaction pathway (details in the SI).

Comparison with other two-metal-dependent enzymes. The mechanism of phosphodiester bond cleavage has been studied in several two-metal-ion enzymes.[13,22,23,31] These studies conveyed on the associative nature of the chemical reaction, which requires the activation of the nucleophile, before the leaving group is released. A recent study of the HIV-1 RNase H,[32] employing a finite-temperature string method and the B3LYP functional, indicated a reaction mechanism similar to our H983-activated catalysis (Figure 2) and similar energetics, strongly supporting our findings.

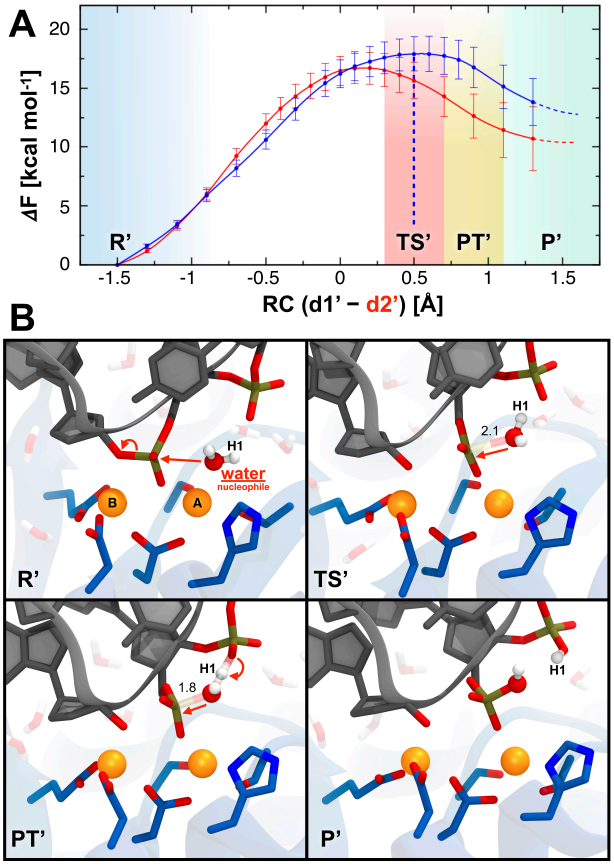

Figure 3. Alternative reaction pathway. (a) Free energy profile (ΔF#) for the phosphate-mediated S_N1 dissociative mechanism (blue line), highlighting regions corresponding to the reactant (R'), transition state (TS'), proton transfer (PT') and products (P'). The free energy profile for the S_N2 associative pathway activated by H893 is also shown (red line). (b) Snapshots of the R', TS', PT' and P' states, as from the S_N1 pathway.

In that study, the proton abstraction by an active site histidine occurs right before the phosphorane $TS^{\ddagger}$ and is barrier-less, analogously to the S_N2 mechanism described here. Our *ab-initio* MD also reveal that a phosphate-mediated activation of the nucleophile leads to a dissociative S_N1 mechanism, which is however energetically disfavored compared to the associative pathway activated by H893 (Figure 3). Here, the deprotonation of the attacking nucleophile oc-

curs after the elimination of the leaving group and does not require a specific base activating the nucleophile. A similar dissociative (and less specific) catalysis has been rarely found in the two-metal-dependent enzymes, as aided by Zn^{2+},[28] or promoted by a non-Mg^{2+}–coordinated water.[29,30] It has been observed in group II intron ribozyme,[25] where a solvent-mediated mechanism has been proposed. However, nucleolytic ribozymes commonly react through an associative catalysis, activated by guanine nucleobases.[33–36] Considering these studies, and that the H893A substitution abolishes the RuvC catalysis,[7] a phosphate-mediated dissociative mechanism is unlikely. Notably, the RuvC site displays remarkable similarity with the RuvC resolvase (Figure S4),[37] which resolves Holliday junctions during genetic recombination and post-replication repair. This suggests a similar histidine-activated S_N2 mechanism, advocating for a common catalytic strategy for genome-editing and recombination. Overall, our *ab-initio* approach characterizes the two-metal aided phosphodiester bond cleavage in RuvC, in agreement with experimental data. Based on this approach, we are investigating the HNH catalysis, which uses a single metal differing from RuvC, to complete our understanding of DNA cleavage by CRISPR-Cas9.

Conclusions

In summary, *ab*-initio QM(Car-Parrinello)/MM MD reveal that CRISPR-Cas9 cleaves the DNA non-target strand through an associative mechanism, activated by H983 and fundamentally assisted by the dynamics of the two catalytic Mg^{2+} ions, which facilitate nucleophile formation, stabilize the $\mathbf{TS}^{\ddagger}$ and enable the leaving group exit. The mechanistic details of this two-Mg^{2+} aided catalysis provide fundamental understanding on how Cas9 cleaves DNA. These valuable insights can be exploited for improving the CRISPR-Cas9 catalytic efficiency and for interfering with its metal-dependent activity, also helping in the development of novel Cas9-based genome-editing tools.

Acknowledgments

We thank Samuel H. Sternberg and Martin Pacesa for useful discussions.

Funding

This material is based upon work supported by the National Science Foundation under Grant No. CHE-1905374. Computer time was provided by the Extreme Science and Engineering Discovery Environment (XSEDE) through the grant No. TG-MCB160059.

References

(1) Doudna, J. A.; Charpentier, E. Genome Editing. The New Frontier of Genome Engineering with CRISPR-Cas9. *Science* **2014**, *346* (6213).

(2) Jinek, M.; Chylinski, K.; Fonfara, I.; Hauer, M.; Doudna, J. A.; Charpentier, E. A Programmable Dual-RNA-Guided DNA Endonuclease in Adaptive Bacterial Immunity. *Science* **2012**, *337*, 816–821.

(3) Sternberg, S. H.; Redding, S.; Jinek, M.; Greene, E. C.; Doudna, J. A. DNA Interrogation by the CRISPR RNA-Guided Endonuclease Cas9. *Nature* **2014**, *507*, 62-67.

(4) Sternberg, S. H.; LaFrance, B.; Kaplan, M.; Doudna, J. A. Conformational Control of DNA Target Cleavage by CRISPR-Cas9. *Nature* **2015**, *527*, 110–113.

(5) Steitz, T. A.; Steitz, J. A. A General Two-Metal-Ion Mechanism for Catalytic RNA. *Proc. Natl. Acad. Sci.* **1993**, *90* (14), 6498–6502.

(6) Jinek, M.; Jiang, F.; Taylor, D. W.; Sternberg, S. H.; Kaya, E.; Ma, E.; Anders, C.; Hauer, M.; Zhou, K.; Lin, S.; et al. Structures of Cas9 Endonucleases Reveal RNA-Mediated Conformational Activation. *Science* **2014**, *343*, 12479911–12479971.

(7) Nishimasu, H.; Ran, F. A.; Hsu, P. D.; Konemann, S.; Shehata, S. I.; Dohmae, N.; Ishitani, R.; Zhang, F.; Nureki, O. Crystal Structure of Cas9 in Complex with Guide RNA and Target DNA. *Cell* **2014**, *156*, 935–949.

(8) Jiang, F. G.; Taylor, D. W.; Chen, J. S.; Kornfeld, J. E.; Zhou, K. H.; Thompson, A. J.; Nogales, E.; Doudna, J. A. Structures of a CRISPR-Cas9 R-Loop Complex Primed for DNA Cleavage. *Science* **2016**, *351*, 867–871.

(9) Anders, C.; Niewoehner, O.; Duerst, A.; Jinek, M. Structural Basis of PAM-Dependent Target DNA Recognition by the Cas9 Endonuclease. *Nature* **2014**, *513*, 569–573.

(10) Palermo, G. Structure and Dynamics of the CRISPR–Cas9 Catalytic Complex. *J. Chem. Inf. Model.* **2019**, *59*, 2394–2406.

(11) Palermo, G.; Miao, Y.; Walker, R. C.; Jinek, M.; McCammon, J. A. CRISPR-Cas9 Conformational Activation as Elucidated from Enhanced Molecular Simulations. *Proc. Natl. Acad. Sci. U. S. A.* **2017**, *114*, 7260–7265.

(12) Zuo, Z.; Liu, J. Cas9-Catalyzed DNA Cleavage Generates Staggered Ends: Evidence from Molecular Dynamics Simulations. *Sci Rep* **2016**, *5*, 37584.

(13) Palermo, G.; Cavalli, A.; Klein, M. L.; Alfonso-Prieto, M.; Dal Peraro, M.; De Vivo, M. Catalytic Metal Ions and Enzymatic Processing of DNA and RNA. *Acc. Chem. Res.* **2015**, *48*, 220–228.

(14) Stephenson, A. A.; Raper, A. T.; Suo, Z. Bidirectional Degradation of DNA Cleavage Products Catalyzed by CRISPR/Cas9. *J. Am. Chem. Soc.* **2018**, *140*, 3743–3750.

(15) Car, R.; Parrinello, M. Unified Approach for Molecular Dynamics and Density-Functional Theory. *Phys. Rev. Lett.* **1985**, *55*, 2471–2474.

(16) Laio, A.; VandeVondele, J.; Rothlisberger, U. A Hamiltonian Electrostatic Coupling Scheme for Hybrid Car–Parrinello Molecular Dynamics Simulations. *J. Chem. Phys.* **2002**, *116*, 6941–6947.

(17) Charles W. Bock, †,‡; Amy Kaufman Katz, †; George D. Markham, † and; Jenny P. Glusker*, †. Manganese as a Replacement for Magnesium and Zinc: Functional

Comparison of the Divalent Ions. **1999**. *J. Am. Chem. Soc.* 121, 7360-7372.

(18) Wedekind, J. E.; Dutta, D.; Belashov, I. A.; Jenkins, J. L. Metalloriboswitches: RNA-Based Inorganic Ion Sensors That Regulate Genes. *J. Biol. Chem.* **2017**, *292*, 9441–9450.

(19) Leonarski, F.; D'Ascenzo, L.; Auffinger, P. Mg^{2+} Ions: Do They Bind to Nucleobase Nitrogens? *Nucleic Acids Res.* **2017**, *45*, 987–1004.

(20) Yang, W. Nucleases: Diversity of Structure, Function and Mechanism. *Q. Rev. Biophys.* **2011**, *44*, 1–93.

(21) Ciccotti, G.; Ferrario, M.; Hynes, J. T.; Kapral, R. Constrained Molecular Dynamics and the Mean Potential for an Ion Pair in a Polar Solvent. *Chem. Phys.* **1989**, *129*, 241–251.

(22) De Vivo, M.; Dal Peraro, M.; Klein, M. L. Phosphodiester Cleavage in Ribonuclease H Occurs via an Associative Two-Metal-Aided Catalytic Mechanism. *J. Am. Chem. Soc.* **2008**, *130*, 10955–10962.

(23) Rosta, E.; Nowotny, M.; Yang, W.; Hummer, G. Catalytic Mechanism of RNA Backbone Cleavage by Ribonuclease H from Quantum Mechanics/Molecular Mechanics Simulations. *J. Am. Chem. Soc.* **2011**, *133*, 8934–8941.

(24) Ivanov, I.; Tainer, J. A.; McCammon, J. A. Unraveling the Three-Metal-Ion Catalytic Mechanism of the DNA Repair Enzyme Endonuclease IV. *Proc. Natl. Acad. Sci. U. S. A.* **2007**, *104*, 1465–1470.

(25) Casalino, L.; Palermo, G.; Rothlisberger, U.; Magistrato, A. Who Activates the Nucleophile in Ribozyme Catalysis? An Answer from the Splicing Mechanism of Group II Introns. *J. Am. Chem. Soc.* **2016**, *138*, 10374–10377.

(26) Palermo, G.; Stenta, M.; Cavalli, A.; Dal Peraro, M.; De Vivo, M. Molecular Simulations Highlight the Role of Metals in Catalysis and Inhibition of Type II Topoisomerase. *J. Chem. Theory Comput.* **2013**, *9*, 857–862.

(27) Gong, S.; Yu, H. H.; Johnson, K. A.; Taylor, D. W. DNA Unwinding Is the Primary Determinant of CRISPR-Cas9 Activity. *Cell Rep.* **2018**, *22*, 359–371.

(28) Ló Pez-Canut, V.; Roca, M.; Bertrán, J.; Moliner, V.; Aki Tuñón, I. Theoretical Study of Phosphodiester Hydrolysis in Nucleotide Pyrophosphatase/Phosphodiesterase. Environmental Effects on the Reaction Mechanism. **2010**, *J. Am. Chem. Soc.* 132, 6955-6963.

(29) Akola, J.; Jones, R. O. Density Functional Calculations of ATP Systems. 2. ATP Hydrolysis at the Active Site of Actin. **2006**. *J. Phys. Chem. B* 110, 8121-8129

(30) Imhof, P.; Fischer, S.; Smith, J. C. Catalytic Mechanism of DNA Backbone Cleavage by the Restriction Enzyme EcoRV: A Quantum Mechanical/Molecular Mechanical Analysis. *Biochemistry* **2009**, *48*, 9061–9075.

(31) Cisneros, G. A.; Perera, L.; Schaaper, R. M.; Pedersen, L. C.; London, R. E.; Pedersen, L. G.; Darden, T. A. Reaction Mechanism of the ε Subunit of *E. Coli* DNA Polymerase III: Insights into Active Site Metal Coordination and Catalytically Significant Residues. *J. Am. Chem. Soc.* **2009**, *131*, 1550–1556.

(32) Dürr, S. L.; Bohuszewicz, O.; Suardiaz, R.; Jambrina, P. G.; Peter, C.; Shao, Y.; Rosta, E. The Dual Role of Histidine as General Base and Recruiter of a Third Metal Ion in HIV-1 RNase H. **2019** ChemRxiv preprint, DOI: 10.26434/chemrxiv.8224538

(33) Wilson, T. J.; Liu, Y.; Lilley, D. M. J. Ribozymes and the Mechanisms That Underlie RNA Catalysis. *Front. Chem. Sci. Eng.* **2016**, *10*, 178–185.

(34) Chen, H.; Giese, T. J.; Golden, B. L.; York, D. M. Divalent Metal Ion Activation of a Guanine General Base in the Hammerhead Ribozyme: Insights from Molecular Simulations. *Biochemistry* **2017**, *56*, 2985–2994.

(35) Mlýnský, V.; Walter, N. G.; Šponer, J.; Otyepka, M.; Banáš, P. The Role of an Active Site Mg(2+) in HDV Ribozyme Self-Cleavage: Insights from QM/MM Calculations. *Phys. Chem. Chem. Phys.* **2015**, *17*, 670–679.

(36) Zhang, S.; Ganguly, A.; Goyal, P.; Bingaman, J. L.; Bevilacqua, P. C.; Hammes-Schiffer, S. Role ofthe Active Site Guanine in the GlmS Ribozyme Self-Cleavage: Quantum Mechanical/Molecular Mechanical Energy Simulations. *J. Am. Chem. Soc.* **2015**, *137*, 784.

(37) Górecka, K. M.; Komorowska, W.; Nowotny, M. Crystal Structure of RuvC Resolvase in Complex with Holliday Junction Substrate. *Nucleic Acids Res.* **2013**, *41*, 9945–9955.